Accepted Manuscript

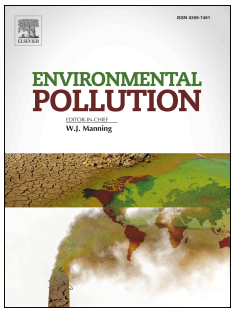

Surface nitrous oxide concentrations and fluxes from water bodies of the agricultural watershed in Eastern China

Qitao Xiao, Zhenghua Hu, Congsheng Fu, Hang Bian, Xuhui Lee, Shutao Chen, Dongyao Shang

PII: S0269-7491(18)35310-7

DOI: https://doi.org/10.1016/j.envpol.2019.04.076

Reference: ENPO 12477

To appear in: *Environmental Pollution*

Received Date: 26 November 2018

Revised Date: 11 April 2019

Accepted Date: 15 April 2019

Please cite this article as: Xiao, Q., Hu, Z., Fu, C., Bian, H., Lee, X., Chen, S., Shang, D., Surface nitrous oxide concentrations and fluxes from water bodies of the agricultural watershed in Eastern China, *Environmental Pollution* (2019), doi: https://doi.org/10.1016/j.envpol.2019.04.076.

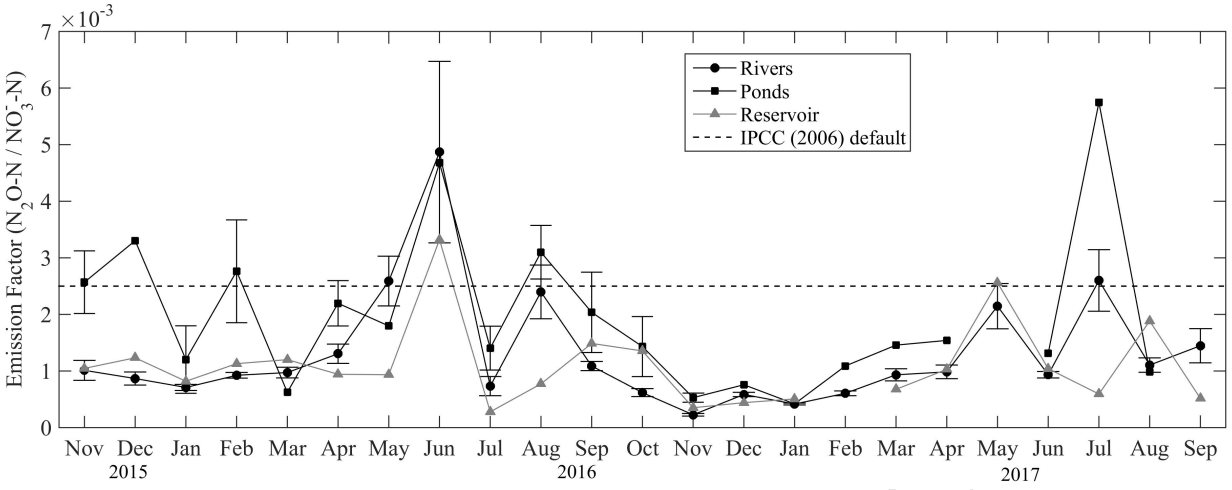

Surface Nitrous Oxide Concentrations and Fluxes from Water Bodies of the Agricultural Watershed in Eastern China

Qitao Xiao[1,2], Zhenghua Hu[1*], Congsheng Fu[2], Hang Bian[1], Xuhui Lee[3,4], Shutao Chen[1], Dongyao Shang[1]

[1]Collaborative Innovation Center on Forecast and Evaluation of Meteorological Disasters, Jiangsu Key Laboratory of Agricultural Meteorology, Nanjing University of Information Science & Technology, Nanjing 210044, China

[2]Key Laboratory of Watershed Geographic Sciences, Nanjing Institute of Geography and Limnology, Chinese Academy of Sciences, Nanjing 210008, China

[3]Yale-NUIST Center on Atmospheric Environment, Nanjing University of Information Science & Technology, Nanjing 210044, China

[4]School of Forestry and Environmental Studies, Yale University, New Haven, Connecticut 06511, USA

[*]**Corresponding author:** Zhenghua Hu

Email: zhhu@nuist.edu.cn

Phone: +86-025-58731193

Address: Collaborative Innovation Center on Forecast and Evaluation of Meteorological Disasters, Jiangsu Key Laboratory of Agricultural Meteorology Nanjing University of Information Science and Technology, 219 Ningliu Road, Nanjing, Jiangsu Province, China

Abstract: Agriculture is one of major emission sources of nitrous oxide (N_2O), an important greenhouse gas dominating stratospheric ozone destruction. However, indirect N_2O emissions from agriculture watershed water surfaces are poorly understood. Here, surface-dissolved N_2O concentration in water bodies of the agricultural watershed in Eastern China, one of the most intensive agricultural regions, was measured over a two-year period. Results showed that the dissolved N_2O concentrations varied in samples taken from different water types, and the annual mean N_2O concentrations for rivers, ponds, reservoir, and ditches were 30±18, 19±7, 16±5 and 58±69 nmol L^{-1}, respectively. The N_2O concentrations can be best predicted by the NO_3^--N concentrations in rivers and by the NH_4^+-N concentrations in ponds. Heavy precipitation induced hot moments of riverine N_2O emissions were observed during farming season. Upstream waters are hot spots, in which the N_2O production rates were two times greater than in non-hotspot locations. The modeled watershed indirect N_2O emission rates were comparable to direct emission from fertilized soil. A rough estimate suggests that indirect N_2O emissions yield approximately 4% of the total N_2O emissions yield from N-fertilizer at the watershed scale. Separate emission factors (EF) established for rivers, ponds, and reservoir were 0.0013, 0.0020, and 0.0012, respectively, indicating that the IPCC (Inter-governmental Panel on Climate Change) default value of 0.0025 may overestimate the indirect N_2O emission from surface water in eastern China. EF was inversely correlated with N loading, highlighting the potential constraints in the IPCC methodology for water with a high anthropogenic N input.

Capsule abstract

The surface indirect N_2O emission rates were comparable to direct emission, but the

IPCC default emission factor may overestimate indirect N_2O emission in the region.

Keywords: Indirect emission; N_2O concentrations; emission rates; emission factor; IPCC

Introduction

Nitrous oxide (N_2O) is a powerful and long-lived greenhouse gas and also a dominant component in the destruction of the stratospheric ozone (Ravishankara et al. 2009). The atmospheric N_2O concentration is estimated to have increased by 22% since 1750, with a current concentration of 329 ppb (Davidson 2009; Cooper et al. 2017). The increasing atmospheric N_2O concentration has received considerable attention. The estimated annual global N_2O emission is 13.3~18.8 Tg N yr^{-1}, to which agriculture contributes nearly 30% (Xu et al. 2008; Cooper et al. 2017). Importantly, agriculture is considered by far the largest source (~80%) of anthropogenic N_2O via both direct emission and indirect emission (Kroeze et al. 1999; Davidson 2009; Cooper et al. 2017).

Anthropogenic N_2O input into the atmosphere from fertilized soils are defined as direct emission, while indirect emission represents N_2O production in ditches, streams, and rivers induced by leaching and runoff of reactive N from agricultural areas (Mosier et al. 1998; Fu et al. 2018). Direct N_2O emissions have been well documented through a large amount of field measurements (Xu et al. 2008; Shcherbak et al. 2014), while indirect emissions from agricultural watershed are less well constrained due to the scarcity of studies on this topic (Reay et al. 2003; Outram and Hiscock; Fu et al. 2018). Importantly, indirect emission is estimated to account for over one-quarter of global total agricultural N_2O emissions (Reay et al. 2012; Venkiteswaran et al. 2014) and dominates the inter-annual variability of total emission (Griffis et al. 2017).

Meanwhile, riverine N_2O emissions, especially in agricultural areas, remain a major source of uncertainty in the global N_2O budget due to the large spatiotemporal variability (Beaulieu et al. 2011; Borges et al. 2015; Audet et al. 2017). More field measurements of indirect N_2O emission are needed to reduce the uncertainty and improve the reliability of the global anthropogenic N_2O budget (Reay et al. 2012; Saikawa et al. 2014).

IPCC provided emission factors (EF) to estimate indirect N_2O emissions resulting from fertilizer-N and manure-N loss via leaching and runoff (De Klein et al. 2006), in which global and regional N_2O emissions from a water body can be calculated by multiplying the nitrogen fertilizer input or relevant anthropogenic N loading with the default EF (Hu et al. 2016; Hama-Aziz et al. 2017; Fu et al. 2018). Since 2006, the IPCC default EF values for rivers, groundwater, and estuaries were both set to 0.0025 (De Klein et al., 2006). However, studies have shown that the default EF is poorly constrained due to high variability in environmental conditions (Turner et al. 2015; Cooper et al. 2017; Griffis et al. 2017). For example, a field measurement showed that the IPCC default EF is underestimated up to nine-fold in rivers in the U.S. Corn Belt, an intensively agricultural region (Turner et al. 2015; Fu et al. 2017; Fu et al. 2018), but it is unexpectedly overestimated in an intensively agriculture area in other regions (Clough et al. 2007; Outram and Hiscock 2012; Hama-Aziz et al. 2017). Using the default IPCC emission factor for predicting indirect N_2O emissions from all rivers may be inappropriate, and more measurements are needed to accurately calculate the

97 EF_{5r} (Outram and Hiscock 2012; Hama-Aziz et al. 2017; Tian et al. 2017).

98

99 Heavy farmland N fertilizer application in Eastern China, one of most intensively
100 agricultural regions in the world, has led to a high N loading input in the watershed.
101 The fertilizer N application rate is up to 600 kg N ha^{-1} yr^{-1} in Eastern China (Ju et al.
102 2009; Xing and Zhu 2002). For comparison, the value is only approximately 100 kg N
103 ha^{-1} yr^{-1} in intensively agricultural regions in the US (Griffis et al. 2017; Turner et al.
104 2015). Further, a large amount of farmland N-fertilizer (~280 kg N ha^{-1} yr^{-1}) enters the
105 watershed via runoff and leaching in Eastern China (Xing and Zhu 2002; Yan et al.
106 2011), which may significantly increase the N_2O production rates (Beaulieu et al.
107 2011). Previous studies suggested that the surface water N_2O emissions in Eastern
108 China may be very high due to the vast farmland N-fertilizer (Seitzinger and Kroeze
109 1998). However, until now, limited information is available regarding the
110 characteristics of watershed N_2O dynamics in this area.

111

112 In this study, we measured the dissolved N_2O concentration in water bodies in a
113 typical agricultural watershed in Eastern China. Our objectives were to quantify the
114 importance of agricultural watershed fueled by farmland N-fertilizer as sources of
115 indirect N_2O emission in this area, to explore the indirect N_2O emission factor, and to
116 further investigate the spatiotemporal characteristics of N_2O dynamics.

117

118 ## 2 Materials and Methods

2.1 Study area

This field measurement was carried out in a typical agriculture watershed located in Eastern China (31°58′ to 32°01′N, 119°12′ to 119°14′E; Figure S1). The watershed has previously been reported in detail (Yan et al. 2011). Briefly, there is a reservoir, three rivers, and thousands of small pond in the watershed. The average annual precipitation is 1100 mm and the mean annual temperature is 15 °C. The major annual cropping rotations are rice-wheat for the paddy fields and maize-rapeseed, respectively. There is no industry in the studied area, and agriculture is the dominant local source of anthropogenic N.

2.2 Sample collection and analysis

A watershed-scale sampling round was conducted in each month from October 2015 to September 2017, during which samples were taken from the surface water of the reservoir, rivers, ponds, and ditches (Figure S1). As a whole, water samples were collected from 30 sampling sites, of which 1 site was in a reservoir, 19 sites were in rivers, 3 sites were in ponds, and 7 sites were in ditches. There are three rivers in the watershed: River 1, River 2, and River 3, respectively. Given the river length, the sampling sites were divided into two sections in River 1 (midstream and downstream) and three sections (upstream, midstream, and downstream) in River 2, respectively. It should be noted that the ditches sometimes dry up without covering water, leading to discontinuous sampling.

Each watershed-scale survey was completed over two consecutive days. The procedures of sampling and analysis have previously been reported in detail in Xiao et al. 2019. Briefly, triplicate bubble-free water samples were collected at a 20-cm depth below the surface using 300 mL glass bottles, and these bottles were transported to lab for dissolved N_2O concentration analysis using the headspace equilibration method. Water samples were also collected using an organic glass hydrophore to the ammonium-nitrogen (NH_4^+-N), nitrate-nitrogen (NO_3^--N), and nitrite-nitrogen (NO_2^--N) analysis by a continuous flow analyzer (Skalar san^{++}, Netherlands). The water temperature, pH, specific conductance (Spc), and dissolved oxygen concentration (DO) were measured *in situ* with a multiparameter probe (YSI 650MDS, YSI Inc. Yellow Springs, OH, USA) at a 20-cm depth to be consistent with water sampling.

2.4 N_2O fluxes and emission factor calculations

The N_2O fluxes (F_n, μmol m^{-2} d^{-1}, positive indications of N_2O emission from water to atmosphere) was calculated using water-air gas exchange model:

$$F_n = k \times (C_w - C_{eq}) \quad (1)$$

where C_w is the surface dissolved N_2O concentration (μmol m^{-3}) in water measured by headspace equilibration method, C_{eq} is the N_2O concentration in water that is in equilibrium with the atmosphere at the *in-situ* temperature, and k is the gas transfer coefficient. For the rivers, k was calculated considering both wind and water turbulence (Clough et al. 2007):

$$k = 2.78E^{-6}au_{10}^2\left(\frac{S_c}{660}\right)^{0.5} + \sqrt{\frac{DU}{h}} \quad (2)$$

where $2.78E^{-6}$ is a conversion factor (cm h^{-1} to m s^{-1}), a is a constant (0.31), u_{10} is the wind speed at a height of 10 m above the water surface, and S_c is the Schmidt number for N_2O, U is the river water velocity (m s^{-1}), h is the average river depth (m), and D is the N_2O diffusion coefficient in the water. The hourly measurement of wind speed was obtained from a weather station in the watershed to calculate the k. The river water velocity is steady and only varies depending upon precipitation (Yan et al. 2011; Xia et al. 2013b).

For the lentic ecosystem (reservoir and ponds), the N_2O transfer velocity is mainly driven by wind speed because no surface water flow occurs. k (cm h^{-1}) was calculated from a wind-dependent formula derived from a small shallow lake as follows (Cole and Caraco 1998):

$$k = (S_c/660)^{-n} \ (2.07 + 0.215 \times u_{10}^{1.7}) \quad (3)$$

There is no separate equation for k calculation for ditches, and Equation (3) was also used for calculating the gas transfer coefficient k for ditches.

The indirect N_2O emission factor (EF) for rivers, ponds, ditches, and the reservoir were calculated using the common IPCC methodology as follows (De Klein et al. 2006):

$$EF = N_2O\text{-}N/NO_3^-\text{-}N \quad (4)$$

Where N_2O−N and NO_3^--N are concentrations measured in rivers, ponds, ditches, and the reservoir. Equation (4) has been widely used to calculate the indirect N_2O

emission factor (Turner et al. 2015; Hama-Aziz et al. 2017; Tian et al. 2017).

2.5 Data analysis

Statistical analyses were conducted with SPSS version 18.0 (SPSS, Inc., USA). In the study area, spring is from March to the end of May, summer is from June to August, autumn is from September to November, and winter is from December to February in next year. Simple linear and multi-linear stepwise regression analyses were performed to determine the relationships among N_2O, the emission factor, and independent variables (e.g., NH_4^+-N, NO_3^--N, and NO_2^--N). The entire two-year dataset was divided according to water type (e.g., rivers, ponds, ditches, and reservoir), and the difference of their mean N_2O concentrations and fluxes was examined using a one-way analysis of variance (ANOVA). After completing the ANOVA test, a least significant difference (LSD) post hoc test was conducted. Differences at $p < 0.05$ were labeled as statistically significant in all analyses.

3 Results

3.1 Physical and chemical characteristics

There was no obvious variation in water temperature across different water body types in the agricultural watershed (Figure 2S(a)). The annual mean water temperature is 19.3 ^oC over the two-year study period. There was a clear seasonality for water temperature, with the highest water temperature appearing in the summer (33.3 ^oC) and the lowest (6.3 ^oC) in winter. The annual mean wind speed was 2.5 m s^{-1} based on

207 the measurement from the local weather station.

208

209 In contrast to water temperature, the surface water chemical properties varied among
210 rivers, ponds, reservoir, and ditches (Table 1 and Figure 2S). Generally, the NO_3^--N
211 concentrations was highest in ditches with annual mean value of 1.85 mg L^{-1},
212 followed by rivers (0.99 mg L^{-1}), reservoir (0.54 mg L^{-1}) and ponds (0.47 mg L^{-1}). In
213 contrast, the highest NH_4^+-N concentration appeared in ponds with annual mean value
214 of 0.32 mg L^{-1}, followed by rivers and reservoirs. The NO_2^--N concentrations in these
215 surface water areas showed minor differences. The average DO concentration was
216 over-saturated only in the reservoir with a value of 10.45 mg L^{-1} or 110% saturation,
217 and the annual mean values for rivers, ponds, and ditches were 6.65, 5.78, and 7.90
218 mg L^{-1}, respectively.

219

220 The NO_3^--N was the dominant form of the total dissolved inorganic nitrogen (DIN) in
221 the surface water of the agricultural watershed (Table 1). For example, the NO_3^--N
222 concentration accounted for 76%, 57%, 72%, and 92% of the total DIN concentration
223 for rivers, ponds, the reservoir, and ditches, respectively. In addition, the surface water
224 NO_3^--N concentrations for the rivers, ponds, and reservoir showed clear seasonality
225 with peak concentrations being observed in summer and winter (Figure 2S(b)),
226 coincides with the crop-planting period. There were no obvious temporal variations
227 for NH_4^+-N concentration except in ponds.

228

3.2 Spatial and temporal characteristics of surface water N_2O concentration

The dissolved N_2O concentration in surface water varied across water body types (Figure S3). Dissolved N_2O concentrations in the ditches spanned a broad range, from 10 to 243 nmol L^{-1}, but varied within relatively narrow ranges of 4-172 nmol L^{-1}, 5-50 nmol L^{-1}, and 9-30 nmol L^{-1} in rivers, pond, and reservoir, respectively. Meanwhile, the annual mean surface N_2O concentration in ditches with a value of 63 nmol L^{-1} was significantly ($p < 0.01$) higher than those in rivers (29 nmol L^{-1}), ponds (20 nmol L^{-1}), and reservoir (15 nmol L^{-1}). The differences of N_2O concentrations between rivers, ponds, and reservoir were insignificant ($p > 0.05$).

The N_2O concentrations also varied within rivers. River 3 with the shortest transport length (Figure S1) had the highest N_2O concentration compared to River 1 and River 2. The overall mean N_2O concentrations were 26, 30, and 35 for rivers 1, 2, and 3, respectively. Further analysis showed large spatial variations for the riverine N_2O concentration along the current direction of the water (Figure S4). A N_2O concentration gradient from the upstream to the estuary is clearly evident. Peak N_2O concentrations were typically found in the upstream of the river. The annual mean N_2O concentrations in upstream, midstream, and downstream of River 2 were 45, 25, and 21 nmol L^{-1}, respectively. River 3 is too short to be sampled at different locations, and samples were only taken from midstream and downstream in River 1, but the measured data also showed that the N_2O concentrations decreased rapidly far from the upstream areas (Figure 4S(b)).

Another notable feature was that the surface N_2O concentration varied over time, especially in rivers. Hot moments, or rapid temporal increases in the surface N_2O concentrations, were evident in rivers (Figure 1). There was clear seasonality for the monthly mean N_2O concentration in rivers, ranging from 15 to 95 nmol L^{-1}, with peak concentrations being observed in the summer. In contrast to rivers, the temporal variation showed a narrower range for ponds (7-34 nmol L^{-1}) and the reservoir (9-30 nmol L^{-1}) but with peak concentrations being observed mostly in the winter. For rivers, the summertime N_2O concentrations with a mean value of 48 nmol L^{-1} were significantly ($p < 0.05$) higher than those in spring (19 nmol L^{-1}), autumn (24 nmol L^{-1}), and winter (28 nmol L^{-1}). For ponds, the summertime N_2O concentration with a mean value of 16 nmol L^{-1} was significant ($p < 0.05$) lower than that in winter (25 nmol L^{-1}). Additionally, the seasonal average values in the reservoir were 13 (spring), 18 (summer), 14 (autumn), and 18 nmol L^{-1} (winter), respectively, showing significant ($p = 0.046$) difference between spring and summer. We cannot characterize the seasonal variation of N_2O concentrations in ditches due to non-continuous measurements in time.

3.3 Relationships between N_2O concentration and environment factors

Surface N_2O concentration in the rivers, ponds, and reservoir exhibited different responses to inorganic N loadings (Figure S5). The N_2O concentration and NO_3^--N concentration exhibited a stronger correlation in rivers ($r = 0.71$, $p < 0.01$) than in

ponds (r = 0.38, p = 0.03). Inversely, a stronger correlation between N_2O concentration and NH_4^+-N concentration was found in ponds (r = 0.65, p < 0.01) than in rivers (r = 0.33, p < 0.01). Additionally, the NO_2^--N concentration was well correlated with the riverine N_2O concentration (r = 0.65, p < 0.01). In the reservoir, the N_2O concentrations showed no significant correlation with any form of inorganic N loadings.

The temporal correlation between the surface water N_2O concentration and water temperature were insignificant for rivers (r = 0.27, p = 0.20), ponds (r = 0.37, p = 0.08), and reservoir (r = 0.11, p = 0.61). Correlation analyses also revealed that the temporal variation in N_2O concentration was not correlated well with the water chemical properties (e.g., Spc, pH, and DO). Precipitation, by contrast, appeared to contribute to the temporal variation of the N_2O concentration (Figure 2). The accumulated precipitation for ten days before sampling was well correlated with the monthly riverine N_2O concentration when the precipitation amounts were greater than 50 mm (r = 0.92, p < 0.01). Importantly, the hot moments, the rapid temporal increase in the riverine N_2O production (Fu et al. 2018), were induced by heavy precipitation during the crop-planting period in the study (Figure 1). However, the temporal correlation between precipitation and the N_2O concentration in the lentic ecosystems (ponds and reservoir) was insignificant (p > 0.05).

3.4 Indirect N_2O fluxes

The mean estimated indirect N_2O emission (mean ± 1 standard deviation) from the surface water of the agricultural watershed was 27.1±23.4 μmol m^{-2} d^{-1} based on two years' field measurements. The rivers were found to have the highest N_2O fluxes, with a mean value of 49.6 μmol m^{-2} d^{-1}. Ditches had the second highest N_2O fluxes with large uncertainly (mean ± 1 standard deviation: 45.2±95.1 μmol m^{-2} d^{-1}; Table 1). The ponds and reservoir showed moderate emission fluxes with a mean value of 8.0 and 5.6 μmol m^{-2} d^{-1}, respectively. The highest N_2O fluxes for the three water body types — rivers, ponds, and reservoir — were found in the summer (Table 1).

The indirect N_2O fluxes from water bodies in the watershed were calculated with the dissolved N_2O concentration. The calculated indirect N_2O fluxes and dissolved N_2O concentration were highly correlated for all records across water body types and over time ($r = 0.97$, $p < 0.01$).The roles of environment factors influencing the N_2O fluxes were similar to those of surface water-dissolved N_2O concentration.

3.5 Indirect N_2O emission factor

The results revealed that the EF was not uniform for the different water types (Figure 3). Ponds had the highest EF, followed by ditches and rivers on average (Table 1). The reservoir, the large water body in the watershed, had the lowest EF with a mean value of 0.0011. The EF of 0.0013 for rivers was nearly half of the default 0.0025 by IPCC. Additionally, the measured EF of 0.0014 for ditches was also significantly lower than the IPCC default value of 0.0025 for river.

317

318 It was evidenced from the field measurements that EF varied over time (Figure 3).
319 The monthly mean EF varied from 0.0002 to 0.0049 for rivers, 0.0004 to 0.0057 for
320 ponds, and 0.0002 to 0.0033 for the reservoir over the two-year period. The riverine
321 EF showed apparent seasonality: summer (mean ± 1 standard deviation:
322 0.0021±0.0016) > spring (0.0015±0.0007) > autumn (0.0009±0.0005) > winter
323 (0.0007±0.0002, Table 1). In contrast to N_2O concentration, the EFs were highly
324 negative with the NO_3^--N concentration for rivers, ponds, and the reservoir (Figure 4).

325

326 # 4 Discussion

327 ## 4.1 Controls on N_2O variability

328 Previous field measurements demonstrated that although other environmental factors
329 such as dissolved oxygen (Kampschreur et al. 2009; Rosamond et al. 2012), organic
330 carbon (Kampschreur et al. 2009), and water temperature (Venkiteswaran et al. 2014)
331 affect the riverine N_2O production rate, the NO_3^--N concentration was the
332 predominant control on the riverine N_2O concentration in this study (Figure S5(a)).
333 The pattern was consistent with previous observations, showing that NO_3^--N is an
334 important driver of riverine N_2O production in agricultural watersheds (Beaulieu et al.
335 2008; Baulch et al. 2011; Turner et al. 2016; Hama-Aziz et al. 2017; Tian et al. 2017).
336 It is likely that farmland N fertilizer loading to rivers stimulates denitrification and
337 associated N_2O production (Kampschreur et al. 2009; Beaulieu et al. 2011; Maavara
338 et al. 2019). NH_4^+-N concentrations, a good indicator of domestic pollution (Garnier

339 et al. 2009), were found to peak in ponds (Table 1). Additionally, the strong
340 relationship between NH_4^+-N and pond N_2O concentration (r = 0.65, p < 0.01; Figure
341 S5(b)) is reasonable because the high NH_4^+-N level may increase the N_2O
342 accumulation via nitrification, which had been demonstrated in high population
343 density areas (Xia et al. 2013a; Yu et al. 2013; Hu et al. 2016). The poor correlation
344 between N_2O and any form of N loading in the reservoir, by contrast, indicated that
345 other biotic and abiotic factors played a greater role than N loading in N_2O production
346 (Deemer et al. 2016).
347
348 Both field measurement and model simulation find that the riverine N_2O production
349 rate is highly sensitive to perturbations in precipitation (Chen et al. 2016; Cooper et al.
350 2017; Griffis et al. 2017; Fu et al. 2018). Here, precipitation (10-day accumulated
351 precipitation prior to sampling > 50 mm) was found to drive the temporal variation of
352 the riverine N_2O concentration (Figure 2a), consistent with previous studies in the
353 agriculture watersheds in Southwestern China (Tian et al. 2017) and UK (Cooper et al.
354 2017). Heavy precipitation is likely to transport more agricultural N loading to the
355 river (Sinha et al. 2017; Figure 2b) and subsequently stimulates N_2O production (Liu
356 and Greaver 2009; Tian et al. 2017). The results reported here showed that heavy
357 precipitation combined with intense agricultural fertilizer application during the
358 farming season triggered riverine N_2O hot moments (Figure 1), which should be
359 captured to reduce the uncertainty of the N_2O budget (Fu et al. 2018; Shrestha and
360 Wang 2018). The projected increase in both heavy and total precipitation induced by

361 climate change (Sinha et al. 2017), together with the increase in the use of nitrogen
362 fertilizer to meet the food demand (Jiang et al. 2010; Saikawa et al. 2014), posed
363 significant potential for agricultural watershed indirect N_2O production in the global
364 N_2O budget.
365
366 Although many previous studies showed a strong positive correlation between
367 temperature and riverine N_2O production (Beaulieu et al. 2010; Hinshaw and
368 Dahlgren 2012; Shrestha and Wang 2018), our results reported here were consistent
369 with the field measurement in a Swedish agricultural catchment showing water
370 temperature had an insignificant effect on seasonal variation of N_2O concentration
371 (Audet et al. 2017). This is probably due to the N concentration outweighs the
372 temperature in determining the water N_2O production via nitrification and
373 denitrification (Kampschreur et al. 2009; Davidson et al. 2015; Capodici et al. 2018).
374 Another notable feature was that the surface NO_3^--N concentration in rivers was the
375 highest in winter, but the highest N_2O concentration occurred in summer in this study
376 (Table 1). Some studies have proposed that the carbon limitation during denitrification
377 is associated with increased N_2O production (Kampschreur et al. 2009; Capodici et al.
378 2018), which may be the explanation for this pattern. Because study has shown that
379 the dissolved organic carbon in these rivers increased from 6.2 mg L^{-1} in summer to
380 18.6 mg L^{-1} in winter, with the C:N ratio increased from 1.3 to 3.1 (Zhao et al. 2013).
381 The high C:N ratio may supply availability carbon sources, resulting in an increase in
382 denitrification efficiency and associated decrease in N_2O production although the high

383 NO_3^--N concentration in winter in this study (Kampschreur et al. 2009; Zhao et al.
384 2013; Capodici et al. 2018).

385

386 The riverine N_2O production rate varies greatly by geographic location (Figure S4).
387 The most notable feature was that the N_2O concentration decreased sharply from the
388 upstream to the estuary, with the mean value decreasing from 47 to 17 nmol L^{-1} in
389 River 2. The result reported here is consistent with the field measurement in other
390 intensive agricultural activity areas, such as the Seine basin in France (Garnier et al.
391 2009), the U.S. Corn Belt (Turner et al. 2015), and a typical agriculture watershed in
392 the UK (Reay et al. 2003). The high NO_3^--N concentrations in upstream waters
393 (Figure 4S(a)), may enhance the microbial processes of N_2O production (Herrman et
394 al. 2008; Zhao et al. 2014). Notably, direct N_2O input from other sources, such as soil
395 and groundwater, might also lead to a high N_2O concentration in upstream waters
396 (Garnier et al. 2009; Beaulieu et al. 2011). As suggested in previous studies, the
397 upstream waters are the hot spot for N_2O production (Peterson et al. 2001; Turner et al.
398 2015). In summary, N_2O production rates in hotspots were two times greater than in
399 non-hotspot locations in the presented study.

400

401 **4.2 Indirect N_2O fluxes in the agricultural watershed**

402 The combined indirect N_2O fluxes from rivers, ponds, and reservoir were calculated
403 to be 383 kg N_2O-N yr^{-1}. The rivers were the most significant contributor of N_2O
404 fluxes of all water bodies, contributing to a total of 161 kg N_2O-N yr^{-1}. Total direct

405 N_2O fluxes from the watershed fertilized soil was estimated to be 12 t (10^3 kg) N yr^{-1}
406 in the watershed (Xia et al. 2013b). Based on a study in another similar region in
407 Eastern China (She et al. 2018), we roughly estimated that the ditch area for the
408 rice-wheat field is 25 hm^2. Adding the annul N_2O emission yield from agriculture
409 ditches (~ 117 kg N_2O-N yr^{-1}) in the watershed, the watershed indirect N_2O emission
410 thus represents approximately 4% of the total N_2O emissions from N-fertilizer.
411 Although the obtained percentage was similar to other studies (Beaulieu et al. 2008;
412 Garnier et al. 2009; Audet et al. 2017), caution should be taken for the following
413 reasons: (1) the ditch areas and N_2O emission rates (45.2±95.1 μmol m^{-2} d^{-1}) had large
414 uncertainly; (2) the presented sampling strategies might omit some riverine emission
415 hot spots and hot moments, which may lead to low biases in the annual total N_2O
416 emission yield (Fu et al. 2018).
417
418 For lentic ecosystems, the annual mean N_2O emission rates in ponds and reservoir
419 (8.0 and 5.6 μmol m^{-2} d^{-1}, respectively) were higher than the median emission rate
420 (3.9 μmol m^{-2} d^{-1}) in global lakes/reservoirs according to Hu *et al*. (2016). Meanwhile,
421 these values were also higher than those in temperature lakes with a mean value of 3.4
422 μmol m^{-2} d^{-1} (Soued et al. 2016). A heavily polluted lake nearby, Lake Taihu, showed
423 a moderate N_2O emission of 3.5 μmol m^{-2} d^{-1} (Xiao et al. 2019). The gas transfer
424 velocity of a lentic ecosystem in the study region can be accurately estimated using
425 the wind-dependent formula, which had been demonstrated previously (Xiao et al.
426 2017). These results together indicated watershed N inputs fueled the pond and

427 reservoir N_2O emission.

428

429 The indirect riverine N_2O fluxes reported here is compared to the results reported by
430 previous studies (Table S1). The literature review in Table S1 showed that the riverine
431 N_2O fluxes across multiple land-use types ranged from 6.7 to 121.3 μmol m^{-2} d^{-1}, with
432 a mean value of 51.3 μmol m^{-2} d^{-1}. Based on a meta-analysis with 169 observations,
433 the global median riverine N_2O emission fluxes is 14.4 μmol m^{-2} d^{-1}, which is
434 significantly lower than the annual mean flux reported here (49.6 μmol m^{-2} d^{-1}). For
435 comparison, the direct N_2O emission rate from fertilized soil in the study area is
436 approximately 60~90 μmol m^{-2} d^{-1} (Zou et al. 2005; Zhou et al. 2014; Liu et al. 2016).
437 Therefore, indirect N_2O emissions caused by N leaching and surface runoff N losses
438 in agriculture watershed could contribute significantly to the total N_2O emission.

439

440 The N_2O emissions from water are often determined by water-air gas exchange model
441 or direct field measurement such as using floating chamber technique (Outram and
442 Hiscock 2012; Zhu et al. 2015; Hama-Aziz et al. 2017; Wu et al. 2018; Capodici et al.
443 2018). The water-air gas exchange model has been frequently employed to quality
444 N_2O emission flux from water, accounting for 80% of flux measurements (Hu et al.
445 2016; Wu et al. 2018), however, the model-based method may either overestimate or
446 underestimate N_2O emission due to the uncertainly in gas transfer coefficient (Yu et al.
447 2013; Raymond et al. 2013; Wu et al. 2018). For comparison, the direct measurement
448 using floating chamber method showed the N_2O emission flux were 48.1-66.1 μmol

449 m^{-2} d^{-1} and below 8.6 μmol m^{-2} d^{-1} from the rivers and ponds, respectively, within the
450 same watershed (Li et al. 2011; Xia et al. 2013a; Han et al. 2014), which were similar
451 to the model-estimated N_2O emission flux in the presented study (river: 49.6 μmol m^{-2}
452 d^{-1}; ponds: 8.0 μmol m^{-2} d^{-1}). Additionally, previous study has shown that the N_2O
453 emission flux measured by the two methods above exhibits the same seasonal
454 variation in an agricultural watershed in southeast China (Wu et al. 2018). Both of
455 these indicate the model-based method was reasonable for quantifying the watershed
456 indirect N_2O emission in this study.
457
458 **4.3 Implication of the measured EF values**
459 This study revealed that indirect N_2O EFs were not uniform for the different surface
460 water types within the same watershed (Table 1 and Figure 3). This is consistent with
461 the field measurement in UK agriculture watershed, which shows that different water
462 types produce various amounts of N_2O (Outram and Hiscock 2012; Hama-Aziz et al.
463 2017). Therefore, separate EFs for each water compartment are required to better
464 understand the indirect N_2O budget. Emission factor for lentic ponds and the reservoir
465 should also be included because our results showed that ignoring the indirect N_2O
466 emission from the lentic ecosystems would lead to an underestimation of the indirect
467 emission yield by 60%.
468
469 For rivers and ditches, the EF values of 0.0013 and 0.0014 were both lower than the
470 IPCC EF value of 0.0025. These results indicated that the IPCC default value of

0.0025 may overestimate the agriculture watershed indirect N_2O emission in the study region. The recent study by Maavara et al. 2019 using mechanistic modeling approach also showed IPCC EFs are likely overestimated. Meanwhile, our data showed that the EF value across different water types varied over time with a peak appearing in the summer (Figure 3), which is consistent with a previous study (Hama-Aziz et al. 2017). Thus, it may be more applicable to have more measurements across different seasons. Meanwhile, we also found that the IPCC approach of using one EF for all rivers may be inappropriate because EFs were highly variable across rivers, as suggested by Beaulieu et al. (2008). The EF values for rivers 1 2, and 3 were 0.0015, 0.0011, and 0.0016, respectively. Since there are no IPCC EFs for the ponds and reservoir (Outram and Hiscock 2012), a comparison cannot be made. However, a synthesis analysis showed that EF for ponds and reservoirs was 0.0012 (Tian et al. 2018), which was significantly lower than that reported EF value of pond (0.0020) but was same as the value of reservoir in this study.

Compared to the previous results, many studies have also observed lower EFs than the IPCC (2006) default value; however, other studies showed higher EFs (Table S1). These inconsistent reports may be reasonable, because a meta-analysis of global data found that riverine N_2O EFs varied across regions (Hu et al. 2016). Meanwhile, our data showed significant negative relationships between EF and N loading (Figure 9), which is consistent with some previous studies (Beaulieu et al. 2011; Hinshaw and Dahlgren 2012; Hu et al. 2016). This can be attributed to decreasing microbial activity

with increasing N input due to progressive biological saturation (Hu et al. 2016; Mulholland et al. 2008). Although previous studies found that large rivers had low EF (Fu et al. 2018; Hinshaw and Dahlgren 2012), we proposed that the lower EF may appear in watersheds with a high anthropogenic N input (Figure 9), highlighting potential constraints in the IPCC methodology for rivers with high N loading. For example, in China, the annual mean riverine N_2O EF in this agriculture watershed with a high N fertilizer rate (~600 kg N ha^{-1} yr^{-1}) was 0.0013, but in the center of the Sichuan Basin with a relatively low N fertilizer rate (~280 kg N ha^{-1} yr^{-1}) (Zhou et al. 2012), the value was 0.0027 (Tian et al. 2017).

5 Conclusions

Two years' field measurements in the watershed, an intensively agricultural region located in Eastern China, showed the surface N_2O concentrations and fluxes varied seasonally and spatially. The annual mean surface dissolved N_2O concentrations for rivers, ponds, reservoir, and ditches were 30 nmol L^{-1}, 19 nmol L^{-1}, 16 nmol L^{-1}, and 58 nmol L^{-1}, corresponding to the computed N_2O fluxes of 49.6 μmol m^{-2} d^{-1}, 8.0 μmol m^{-2} d^{-1}, 5.6 μmol m^{-2} d^{-1}, and 45.2 μmol m^{-2} d^{-1}, respectively.

Dissolved N_2O concentration can be best predicted by NO_3^--N concentrations in rivers ($r = 0.71$, $p < 0.02$) and by NH_4^+ in ponds ($r = 0.65$, $p < 0.01$). The temporal variation of the riverine N_2O concentration appears to be controlled by precipitation, and heavy precipitation induced the emission hot moments during the farming season.

Upstream waters are the hot spots in which riverine N_2O production rates were two times greater than in non-hotspot locations.

The modeled watershed indirect N_2O emission fluxes were comparable to the direct emission fluxes from the fertilized soils. A coarse estimate suggests that indirect N_2O emissions represent approximately 4% of the total N_2O emissions from N-fertilizer at the watershed scale. However, the IPCC default value of 0.0025 may overestimate the agriculture watershed indirect N_2O emission in the study region. We propose that separate EFs for different seasons and different water types may be more appropriate due to the large variability.

Acknowledgements

This study was supported jointly by the National Natural Science Foundation of China (41775152, 41775151, 41801093) and Projected Funded by China Postdoctoral Science Foundation (2018M632404). We thank the staff of the Yale-NUIST Center on Atmospheric Environment for their assistance with field sample collection and laboratory measurements.

References:

Audet, J., M. B. Wallin, K. Kyllmar, S. Andersson, and K. Bishop. 2017. Nitrous oxide emissions from streams in a Swedish agricultural catchment. Agric. Ecosyst. Environ. **236:** 295-303.

Baulch, H. M., S. L. Schiff, R. Maranger, and P. J. Dillon. 2011. Nitrogen enrichment and the emission of nitrous oxide from streams. Global Biogeochem. Cycles. **25**.

Beaulieu, J. J., C. P. Arango, S. K. Hamilton, and J. L. Tank. 2008. The production and emission of

nitrous oxide from headwater streams in the Midwestern United States. Global Change Biol. **14:** 878-894.

Beaulieu, J. J., W. D. Shuster, and J. A. Rebholz. 2010. Nitrous Oxide Emissions from a Large, Impounded River: The Ohio River. Environ. Sci. Technol. **44:** 7527-7533.

Beaulieu, J. J. and others 2011. Nitrous oxide emission from denitrification in stream and river networks. Proc. Natl. Acad. Sci. U.S.A. **108:** 214-219.

Borges, A. V. and others 2015. Globally significant greenhouse-gas emissions from African inland waters. Nat. Geosci. **8:** 637-642.

Capodici, M., A. Avona, V. A. Laudicina, G. Viviani. 2018. Biological groundwater denitrification systems: Lab-scale trials aimed at nitrous oxide production and emission assessment. Sci. Total Environ. **630**: 462-468.

Chen, Z. and others 2016. Partitioning N_2O emissions within the US Corn Belt using an inverse modeling approach. Global Biogeochem. Cycles. **30:** 1192-1205.

Clough, T. J., L. E. Buckthought, F. M. Kelliher, and R. R. Sherlock. 2007. Diurnal fluctuations of dissolved nitrous oxide (N_2O) concentrations and estimates of N_2O emissions from a spring-fed river: implications for IPCC methodology. Global Change Biol. **13:** 1016-1027.

Cole, J. J., and N. F. Caraco. 1998. Atmospheric exchange of carbon dioxide in a low‐wind oligotrophic lake measured by the addition of SF_6. Limnol. Oceanogr. **43:** 647-656.

Cooper, R. J., S. K. Wexler, C. A. Adams, and K. M. Hiscock. 2017. Hydrogeological controls on regional-scale indirect nitrous oxide emission factors for rivers. Environ. Sci. Technol. **51:** 10440-10448.

Davidson, E. A. 2009. The contribution of manure and fertilizer nitrogen to atmospheric nitrous oxide since 1860. Nat. Geosci. **2:** 659-662.

Davidson, T. A. and others 2015. Eutrophication effects on greenhouse gas fluxes from shallow-lake mesocosms override those of climate warming. Global Change Biol. **21:** 4449-4463.

De Klein, C. and others 2006. N_2O emissions from managed soils, and CO_2 emissions from lime and urea application. IPCC Guidelines for National Greenhouse Gas Inventories, Prepared by the National Greenhouse Gas Inventories Programme **4:** 1-54.

Deemer, B. R. and others 2016. Greenhouse Gas Emissions from Reservoir Water Surfaces: A New Global Synthesis. BioScience **66:** 949-964.

Fu, C., X. Lee, T. J. Griffis, J. M. Baker, and P. A. Turner. 2018. A modeling study of direct and indirect N_2O emissions from a representative catchment in the U.S. Corn Belt. Water Resour. Res. **54**.

Fu, C., X. Lee, T. J. Griffis, E. J. Dlugokencky, and A. E. Andrews. 2017. Investigation of the N_2O emission strength in the U. S. Corn Belt. Atmos. Res. **194:** 66-77.

Garnier, J. and others 2009. Nitrous oxide (N_2O) in the Seine river and basin: Observations and budgets. Agric. Ecosyst. Environ. **133:** 223-233.

Griffis, T. J. and others 2017. Nitrous oxide emissions are enhanced in a warmer and wetter world. Proc. Natl. Acad. Sci. U.S.A. **114:** 12081-12085.

Hama-Aziz, Z. Q., K. M. Hiscock, and R. J. Cooper. 2017. Indirect Nitrous Oxide Emission Factors for Agricultural Field Drains and Headwater Streams. Environ. Sci. Technol. **51:** 301-307.

Han, Y., Y. Zheng, R. Wu, J. Yin, and X. Sun. 2014. Nitrous oxide flux at the water-air interface of the river in Nanjing during summer. Environmental Science **35**: 348-355 (In Chinese).

Herrman, K. S., V. Bouchard, and R. H. Moore. 2008. Factors affecting denitrification in agricultural headwater streams in Northeast Ohio, USA. Hydrobiologia **598:** 305-314.

585 Hinshaw, S. E., and R. A. Dahlgren. 2012. Dissolved nitrous oxide concentrations and fluxes from the
586 eutrophic San Joaquin River, California. Environ Sci Technol **47:** 1313-1322.
587 Hu, M., D. Chen, and R. A. Dahlgren. 2016. Modeling nitrous oxide emission from rivers: a global
588 assessment. Global Change Biol. **22:** 3566-3582.
589 Jiang, J., Z. Hu, W. Sun, and Y. Huang. 2010. Nitrous oxide emissions from Chinese cropland fertilized
590 with a range of slow-release nitrogen compounds. Agric. Ecosyst. Environ. **135:** 216-225.
591 Ju, X. T. and others 2009. Reducing environmental risk by improving N management in intensive
592 Chinese agricultural systems. Proc. Natl. Acad. Sci. U.S.A.**106:** 3041-3046.
593 Kampschreur, M., H. Temmink, R. Kleerebezem, M. Jetten, and M. Loosdrecht. 2009. Nitrous oxide
594 emission during wastewater treatment. Water Res. **43**: 4093-4103.
595 Kroeze, C., A. Mosier, and L. Bouwman. 1999. Closing the global N_2O budget: A retrospective analysis
596 1500-1994. Global Biogeochem. Cycles. **13:** 1-8.
597 Li, F., J. Wang, X. Li, X. Xiao, H. Zou, F. Li. 2011. N_2O emission from pond and river in the
598 agricultural watershed of Jurong reservoir, Jiangsu Province. Acta Scientiae Circumstantiae 31:
599 2022-2027 (In Chinese).
600 Liu, L., and T. L. Greaver. 2009. A review of nitrogen enrichment effects on three biogenic GHGs: the
601 CO2 sink may be largely offset by stimulated N_2O and CH_4 emission. Ecol. Lett. **12:**
602 1103-1117.
603 Liu, S., Z. Hu, S. Wu, S. Li, Z. Li, and J. Zou. 2016. Methane and Nitrous Oxide Emissions Reduced
604 Following Conversion of Rice Paddies to Inland Crab Fish Aquaculture in Southeast China.
605 Environ. Sci. Technol. **50:** 633-642.
606 Maavara T, R. Lauerwald, G. Laruelle, Z. Akbarzadeh, N. Bouskill, P. Cappellen, P. Regnier. 2019.
607 Nitrous oxide emissions from inland waters: Are IPCC estimates too high? Global Change
608 Biol. **25**: 473-488.
609 Mosier, A., C. Kroeze, C. Nevison, O. Oenema, S. Seitzinger, and O. van Cleemput. 1998. Closing the
610 global N_2O budget: nitrous oxide emissions through the agricultural nitrogen cycle. Nutr. Cycl.
611 Agroecosyst. **52:** 225-248.
612 Mulholland, P. J. and others 2008. Stream denitrification across biomes and its response to
613 anthropogenic nitrate loading. Nature **452:** 202-205.
614 Outram, F. N., and K. M. Hiscock. 2012. Indirect nitrous oxide emissions from surface water bodies in
615 a lowland arable catchment: a significant contribution to agricultural greenhouse gas budgets?
616 Environ. Sci. Technol. **46:** 8156-8163.
617 Peterson, B. J. and others 2001. Control of nitrogen export from watersheds by headwater streams.
618 Science **292:** 86-90.
619 Ravishankara, A. R., J. S. Daniel, and R. W. Portmann. 2009. Nitrous oxide (N_2O): the dominant
620 ozone-depleting substance emitted in the 21st century. Science **326:** 123-125.
621 Raymond, P. A. and others 2013. Global carbon dioxide emissions from inland waters. Nature **503:**
622 355-359.
623 Reay, D. S. and others 2012. Global agriculture and nitrous oxide emissions. Nat. Clim. Chang. **2:**
624 410-416.
625 Reay, D. S., K. A. Smith, and A. C. Edwards. 2003. Nitrous oxide emission from agricultural drainage
626 waters. Global Change Biol. **9:** 195-203.
627 Rosamond, M. S., S. J. Thuss, and S. L. Schiff. 2012. Dependence of riverine nitrous oxide emissions
628 on dissolved oxygen levels. Nat. Geosci. **5:** 715-718.

Saikawa, E. and others 2014. Global and regional emissions estimates for N_2O. Atmos. Chem. Phys. **14:** 4617-4641.

Seitzinger, S. P., and C. Kroeze. 1998. Global distribution of nitrous oxide production and N inputs in freshwater and coastal marine ecosystems. Global Biogeochem. Cycles. **12:** 93-113.

Shcherbak, I., N. Millar, and G. P. Robertson. 2014. Global metaanalysis of the nonlinear response of soil nitrous oxide (N_2O) emissions to fertilizer nitrogen. Proc. Natl. Acad. Sci. U.S.A. **111:** 9199-9204.

She, D. and others 2018. Limited N removal by denitrification in agricultural drainage ditches in the Taihu Lake region of China. J. Soil. Sediment. **18:** 1110-1119.

Shrestha, N. K., and J. Wang. 2018. Current and future hot-spots and hot-moments of nitrous oxide emission in a cold climate river basin. Environ. Pollut. **239:** 648-660.

Sinha, E., A. M. Michalak, and V. Balaji. 2017. Eutrophication will increase during the 21st century as a result of precipitation changes. Science **357:** 405-408.

Soued, C., P. A. del Giorgio, and R. Maranger. 2016. Nitrous oxide sinks and emissions in boreal aquatic networks in Québec. Nat. Geosci. **9:** 116-120.

Tian, L., Y. Cai, and H. Akiyama. 2018. A review of indirect N_2O emission factors from agricultural nitrogen leaching and runoff to update of the default IPCC values. Environ. Pollut. **245:** 300-306.

Tian, L. L., B. Zhu, and H. Akiyama. 2017. Seasonal variations in indirect N_2O emissions from an agricultural headwater ditch. Biol. Fertil. Soils **53:** 651-662.

Turner, P. A. and others 2016. Regional-scale controls on dissolved nitrous oxide in the Upper Mississippi River. Geophys. Res. Lett. **43:** 4400-4407.

Turner, P. A., T. J. Griffis, X. Lee, J. M. Baker, R. T. Venterea, and J. D. Wood. 2015. Indirect nitrous oxide emissions from streams within the US Corn Belt scale with stream order. Proc. Natl. Acad. Sci. U.S.A. **112:** 9839-9843.

Venkiteswaran, J. J., M. S. Rosamond, and S. L. Schiff. 2014. Nonlinear Response of Riverine N2O Fluxes to Oxygen and Temperature. Environ. Sci. Technol. **48:** 1566-1573.

Wu, S., J. Chen, C. Li, D. Kong, K. Yu, S. Liu, J. Zou. 2018. Diel and seasonal nitrous oxide fluxes determined by floating chamber and gas transfer equation methods in agricultural irrigation watersheds in southeast China. Environ. Monit. Assess. 190:122.

Xia, Y., Y. Li, X. Li, M. Guo, D. She, and X. Yan. 2013a. Diurnal pattern in nitrous oxide emissions from a sewage-enriched river. Chemosphere **92:** 421-428.

Xia, Y. Q., Y. F. Li, C. P. Ti, X. B. Li, Y. Q. Zhao, and X. Y. Yan. 2013b. Is indirect N_2O emission a significant contributor to the agricultural greenhouse gas budget? A case study of a rice paddy-dominated agricultural watershed in eastern China. Atmos. Environ. **77:** 943-950.

Xiao, Q. and others 2017. Spatial variations of methane emission in a large shallow eutrophic lake in subtropical climate. J. Geophys. Res.-Biogeo. **122:** 1597-1614.

Xiao, Q., Xu, X., Zhang, M., Duan, H., Hu, Z., Wang, W., Xiao, W., Lee, X., 2019. Coregulation of nitrous oxide emissions by nitrogen and temperature in China's third largest freshwater lake (Lake Taihu). Limnol. Oceanogr., doi: 10.1002/lno.11098.

Xing, G. X., and Z. L. Zhu. 2002. Regional nitrogen budgets for China and its major watersheds. Biogeochemistry **57:** 405-427.

Xu, X., H. Tian, and D. Hui. 2008. Convergence in the relationship of CO_2 and N_2O exchanges between soil and atmosphere within terrestrial ecosystems. Global Change Biol. **14:** 1651-1660.

673 Yan, X. and others 2011. Nitrogen budget and riverine nitrogen output in a rice paddy dominated
674 agricultural watershed in eastern China. Biogeochemistry **106:** 489-501.
675 Yu, Z. and others 2013. Nitrous oxide emissions in the Shanghai river network: implications for the
676 effects of urban sewage and IPCC methodology. Global Change Biol. **19:** 2999-3010.
677 Zhao, Y., Y. Xia, B. Li, and X. Yan. 2014. Influence of environmental factors on net N_2 and N_2O
678 production in sediment of freshwater rivers. Environ. Sci. Pollut. R. **21:** 9973-9982.
679 Zhao, Y., Y. Xia, T. Kana, Y. Wu, X. Li, X. Yan. 2013. Seasonal variation and controlling factors of
680 anaerobic ammonium oxidation in freshwater river sediments in the Taihu Lake region of
681 China. Chemosphere **93**: 2124-2131.
682 Zhou, F. and others 2014. A new high-resolution N_2O emission inventory for China in 2008. Environ.
683 Sci. Technol. **48:** 8538-8547.
684 Zhou, M. and others 2012. Nitrate leaching, direct and indirect nitrous oxide fluxes from sloping
685 cropland in the purple soil area, southwestern China. Environ. Pollut. **162:** 361-368.
686 Zhu, D., and others. 2015. Nitrous oxide emission from infralittoral zone and pelagic zone in a shallow
687 lake: Implications for whole lake flux estimation and lake restoration. Ecol. Eng. **82**: 368–375.
688 Zou, J. W., Y. Huang, J. Y. Jiang, X. H. Zheng, and R. L. Sass. 2005. A 3-year field measurement of
689 methane and nitrous oxide emissions from rice paddies in China: Effects of water regime, crop
690 residue, and fertilizer application. Global Biogeochem. Cycles. **19**.
691
692

693 **Table 1.** Summary of the dissolved inorganic concentration (NO_3^--N and NH_4^+-N),

694 N_2O concentration and fluxes, and N_2O emission factor (EF) in all collected samples.

695 The presented values are the mean ± standard deviation.

Sample type	Season	NH_4^+-N (mg L^{-1})	NO_3^--N (mg L^{-1})	N_2O concentration (nmol L^{-1})	N_2O flux (μmol m^{-2} d^{-1})	EF
Rivers	overall	0.26±0.15	0.99±0.59	30±18	49.6±55.8	0.0013±0.0010
	spring	0.16±0.05	0.49±0.21	19±3	26.3±12.4	0.0015±0.0007
	summer	0.34±0.15	1.17±0.94	48±28	107.9±90.4	0.0021±0.0016
	autumn	0.24±0.13	1.03±0.38	24±8	31.3±18.4	0.0009±0.0005
	winter	0.30±0.21	1.26±0.27	28±4	32.8±13.0	0.0007±0.0002
Ponds	overall	0.32±0.40	0.47±0.46	19±7	8.0±8.6	0.0020±0.0014
	spring	0.34±0.43	0.39±0.33	16±3	5.8±2.0	0.0015±0.0006
	summer	0.37±0.54	0.20±0.10	16±10	11.9±15.9	0.0029±0.0020
	autumn	0.25±0.24	0.50±0.19	20±7	7.9±5.9	0.0016±0.0009
	winter	0.31±0.39	0.79±0.73	25±5	6.0±3.1	0.0016±0.0011
Reservoir	overall	0.19±0.09	0.54±0.33	16±5	5.6±5.5	0.0011±0.0007
	spring	0.17±0.04	0.35±0.15	13±3	2.8±2.0	0.0012±0.0007
	summer	0.24±0.07	0.58±0.44	18±8	12.3±6.9	0.0013±0.0011
	autumn	0.18±0.14	0.56±0.34	14±2	3.7±2.1	0.0010±0.0005
	winter	0.14±0.07	0.70±0.29	18±2	3.0±2.4	0.0008±0.0004
Ditches	overall	0.12±0.15	1.85±1.81	58±69	45.2±95.1	0.0014±0.0013

Figure 1. Mean surface N_2O concentration and calculated N_2O flux for rivers, ponds, and reservoir during the two-year period. Error bars represent standard error. The symbols in the boxes indicate the hot moments for N_2O, in which samples were collected from rivers after heavy precipitation during the farming season.

Figure 2. Temporal correlation between precipitation and mean concentrations of N_2O and NO_3^--N in rivers. Note that the precipitation was the 10-day accumulated precipitation for each rainfall event before sampling. We assumed that major N losses from croplands induced by heavy rainfall might be transported to the rivers within 10 days based on a previous study (Yan *et al*., 2011)

Figure 3. Temporal variability in the mean emission factor (N_2O-N/NO_3^--N ratio) for rivers, ponds, and reservoir samples collected from November 2015 to September 2017.

Figure 4. Simple liner regression of normalized monthly mean N_2O emission factor (N_2O-N/NO_3^--N ratio) and normalized NO_3^--N concentration in the collected rivers, ponds, and reservoir samples.

715 **Figure 1.** Mean surface N_2O concentration and calculated N_2O flux for rivers, ponds,
716 and reservoir during the two-year period. Error bars represent standard error. The
717 symbols in the boxes indicate the hot moments for N_2O, in which samples were
718 collected from rivers after heavy precipitation during the farming season.

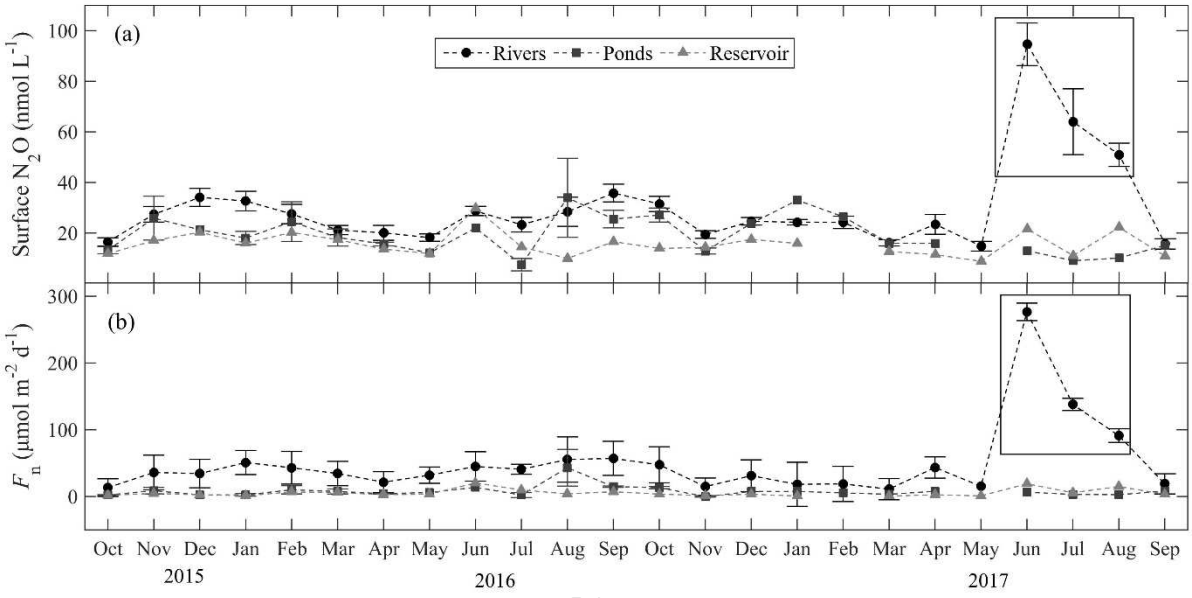

719
720

721 **Figure 2.** Temporal correlation between precipitation and mean concentrations of

722 N_2O and NO_3^--N in rivers. Note that the precipitation was the 10-day accumulated

723 precipitation for each rainfall event before sampling. We assumed that major N losses

724 from croplands induced by heavy rainfall might be transported to the rivers within 10

725 days based on a previous study (Yan *et al*., 2011)

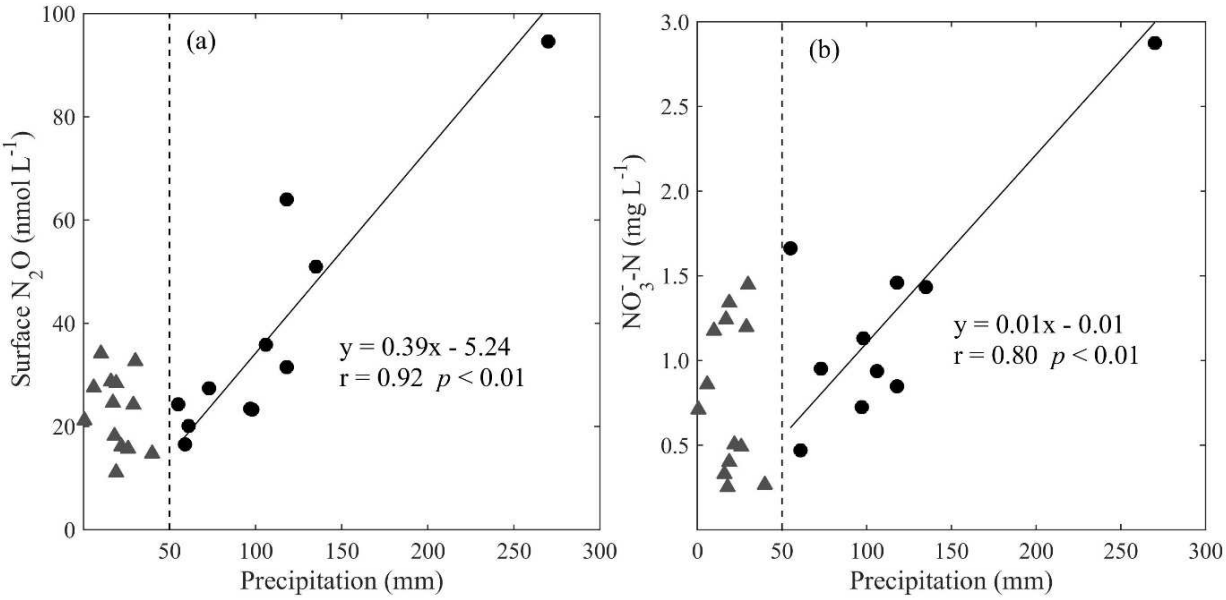

726

727

728 **Figure 3.** Temporal variability in the mean emission factor (N_2O-N/NO_3^--N ratio) for

729 rivers, ponds, and reservoir samples collected from November 2015 to September

730 2017.

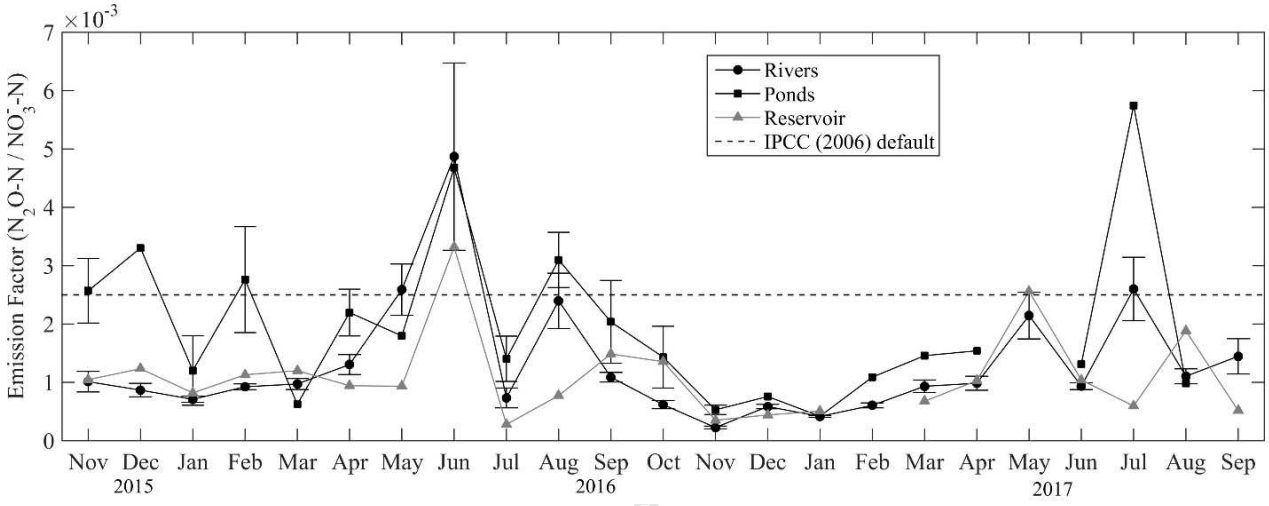

731

732

733 **Figure 4.** Simple liner regression of normalized monthly mean N_2O emission factor

734 (N_2O-N/NO_3^--N ratio) and normalized NO_3^--N concentration in the collected rivers,

735 ponds, and reservoir samples.

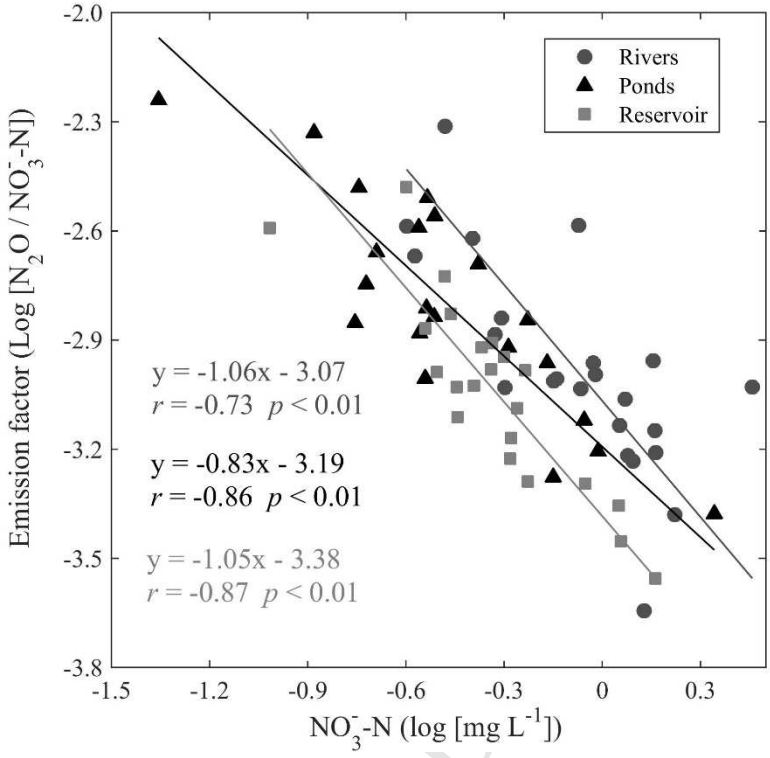

736

- N_2O dynamics in water bodies of the agricultural watershed in eastern China, one intensive agricultural regions with heavy N fertilizer application, were investigated over a two-year period.
- Surface N_2O concentrations and fluxes varied seasonally and spatially, which can be best predicted by N loadings and precipitation.
- The modeled watershed indirect N_2O emission rates were comparable to direct emission from fertilized soil.
- IPCC method may overestimate the indirect N_2O emission from agricultural watershed in eastern China.